

How does the concentration of *malonic acid* affect the average oscillation time of a *manganese* catalyzed Belousov Zhabotinsky reaction?

# Contents

Section	Title	Page
1.0	Introduction	2
1.1	Research Question	
2.0	Background Information	4
2.1	The FKN Mechanism	
2.2	The Oregonator	
3.0	Method	9
3.1	Preliminary Preparations	
3.2	Trial Procedure	
4.0	Results	11
4.1	Sample Calculations	
5.0	Analysis	14
5.1	Pearson's Correlation Coefficient	
5.2	Solution Acidity Adjustments	
5.3	Oregonator Model Comparisons	
6.0	Conclusions	20
6.1	Error Analysis	
7.0	Works Cited	23
8.0	Appendices	25

# Introduction

This experiment has investigated the occurrence of oscillatory variance within the *manganese* catalyzed Belousov Zhabotinsky reaction, and has attempted to answer the question of how a change in the concentration of *malonic acid* affects the oscillation time of this reaction. Belousov Zhabotinsky reactions, which will now be referred to as BZ reactions, are a group of reactions involving an organic acid, *bromate* and *bromide* ions, and a transition metal ion catalyst (Field et al; Shakhshiri). In the case of this essay, the catalyst was the  $Mn^{+2}$  ion, who's concentration was kept constant throughout trials, along with the *bromate* ion.

Due to limitations on the availability of chemicals, this experiment primarily focussed on the BZ reaction within a one dimensional frame, and trials were conducted within a continuously stirred erlenmeyer flask. Other catalysts can be used, though their change in oxidation state during the course of the BZ reaction must be drastic enough such that it is observable even in a thin layer of solution in a petri dish in order for the two dimensional frame to be viable. These alternate catalysts include *cerium III sulphate* and *phenanthroline ferrous II sulphate*, or *ferroin*. Oscillations were induced by simply introducing the  $MnSO_4 \cdot H_2O$  into the solution, and they began after initially generating a red color. The origin of the red, maroon color of the solution when undergoing oscillation is currently disputed by the literature, with some sources claiming the red color originates from bromine dissolved with induced dipoles within water, and others maintaining the color is produced by  $Mn^{+2}$  (Shakhshiri).

Each trial was recorded and reviewed using video editing software, in which individual oscillation times were recorded. Averages were taken of the first five oscillations following the

appearance of red in solution with the addition of  $MnSO_4 \cdot H_2O$ . Only the first five oscillation times were chosen because the reaction slows beyond the fifth oscillation due to depleting amounts of reactants.

Data was collected in the range of  $0.06 \text{ mol dm}^{-3}$  to  $0.24 \text{ mol dm}^{-3}$ , increasing in increments of  $0.02 \text{ mol dm}^{-3}$  for a total of 10 different concentrations of *malonic acid*, with 3 trials of each concentration. The concentration versus average oscillation time graph shows a strong inverse relationship. The data obtained was in support of a negative correlation between  $[CH_2(COOH)_2]$  and the average of the first five oscillations, and the model and simple observation of the elementary stoichiometries show agreement with this. Furthermore, where discrepancies between experimental observation and the model were present, an explanation from the complex ions and oxidation states of the transition metal catalysts was given.

## Research Question

How does the concentration of *malonic acid* affect the oscillation time of a *manganese* catalyzed Belousov Zhabotinsky reaction?

## Background Information

BZ reactions are one of the first examples of oscillatory chemical reactions (Hill and Morgan). All of these reactions share common features, those being a transition metal ion catalyzing oxidation of various, usually organic acids by means of a bromic acid within an acidic water solution (Hill and Morgan). These reactions are important beyond passing scientific fascination, as they remain far from their equilibrium points for significant lengths of time, demonstrating that chemical reactions do not have to be dominated by equilibrium thermodynamic behavior (Hill and Morgan).

If carried out in petri dishes and left unstirred, BZ reactions will generate small coloured spots which evolve into trigger waves emanating from various nucleation points (Hill and Morgan). These nucleation points can be spontaneously generated due to the solution being overly excitable or can be manually induced using a *silver* wire extending from the positive lead of a battery (Hill and Morgan). Existing literature does not explain why this method works, though it may be that the *Ag* is ionized, thus reducing *bromate* in its vicinity, beginning the reaction (Hill and Morgan). When the reaction nucleates at a point, diffusion draws  $Br^-$  from the surrounding regions towards the nucleation point, which causes the process of oxidizing the metal catalyst to dominate, perpetuating the front of lower  $[Br^-]$ . Thus a circular wave is generated, emanating outwards from the point of origin (Hill and Morgan). If the solution is able to support more oscillations, which it will unless extremely depleted of key reactants, concentric rings of trigger waves will form, each annihilating once reaching the container walls (Hill and Morgan).

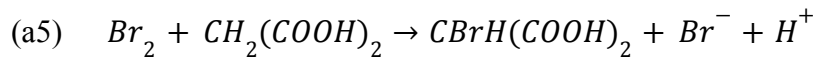
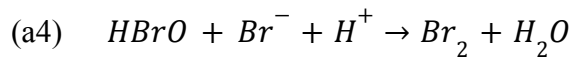
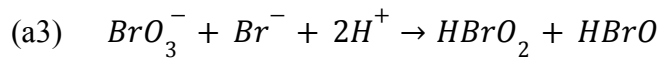
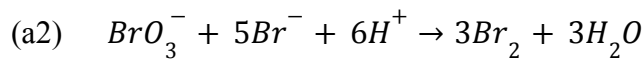
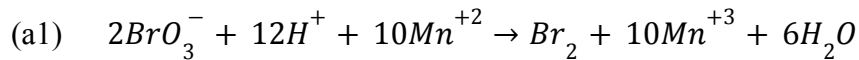
The velocity of any given trigger wave is given by the following equation, determined experimentally (Field et al; Hill and Morgan):

$$v = \{ (0.04) \cdot \sqrt{[H^+][BrO_3^-]} \} cm^2 s^{-1} mol^{-1} dm^3$$

Systems of chemical oscillators are also of great interest in biological systems, which was the initial inspiration for this experiment. BZ trigger waves are of particular notoriety, with examples ranging from the sinoatrial node, the organic pacemaker, causing electrical waves which propagate much like BZ waves to the generation of cyclic adenosine monophosphate in slime mold colonies causing spiral patterns nearly identical to those of the BZ reaction (Epstein and Pojman). RNA has also been found to self-replicate, with fronts of increased RNA concentration moving outward via diffusion (Epstein and Pojman).

## The FKN Mechanism

Modern understanding of the BZ reaction largely stems from the FKN mechanism, which consists of ten major reactions, with the assumption that *malonic acid* will only be monobrominated. These key reactions are as follows (Hill and Morgan; Tyson):



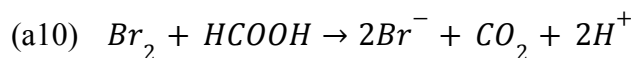
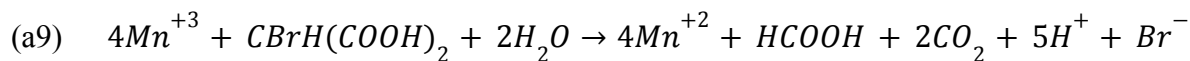
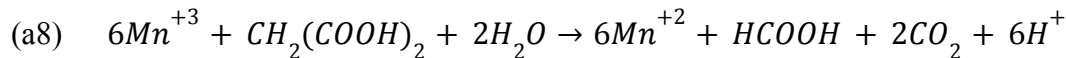
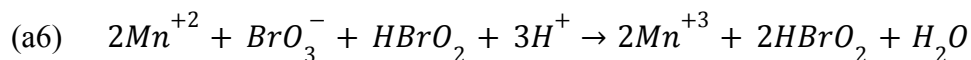
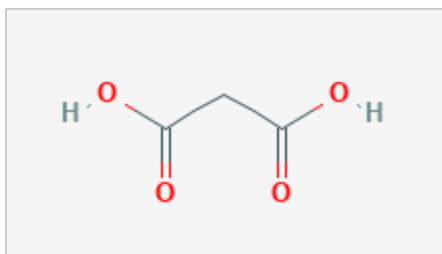


Figure 2.0: Simplified lewis diagram of *malonic acid* (“Malonic Acid”)

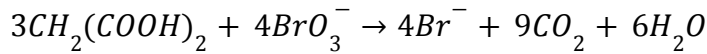


Once the catalyst has been introduced to the solution containing all the other reactants necessary, process (a1) begins to reduce the  $BrO_3^-$  ions into elemental  $Br_2$ , which is followed by process (a5) brominating the *malonic acid*. The reduction of  $BrO_3^-$  is only dominated by process (a1) before the involvement of  $Br^-$  or  $HBrO_2$  (Britton; Shakhshiri). With the introduction of oxidized  $Mn^{+3}$ , *malonic acid* and *bromomalonic acid* are involved in the redox reactions of processes (a8) and (a9), with the complete oxidation of *malonic acid* ending with process (a10) (Hill and Morgan).

With the now present  $Br^-$ , processes (a2), (a3) and (a4) begin to lower  $[Br^-]$  and increase  $[Br_2]$ , beginning the bromination of *malonic acid* in process (a5). In fact, (a3) has been identified by Blandamer et al. to be the process that most influences the frequency of oscillations (Bánsági et al). Process (a2) dominates the reduction of  $BrO_3^-$  when  $[Br^-]$  is high and process (6) when  $[Br$

] is low. With processes (a2) through (a4), we see that  $BrO_3^-$  and  $Br^-$  are being rapidly consumed to feed process (a5) with the bromination of *malonic acid* (Hill and Morgan).

Once  $[Br^-]$  has been sufficiently lowered, process (a6) takes over the reduction of  $BrO_3^-$  and causes an exponential increase of  $HBrO_2$  and the oxidized metal catalyst. Process (a7) begins the instant  $HBrO_2$  is introduced, and eventually completely limits the exponential increase from the autocatalytic production of  $HBrO_2$ . With the newly formed  $Mn^{+3}$  ions, processes (a8), (a9), and (a10) are able to begin oxidizing *malonic acid* while reproducing  $Br^-$ . Once  $[Br^-]$  reaches a critical mass, the reduction of  $BrO_3^-$  is once again dominated by process (a2), and the reaction restarts (Hill and Morgan). Therefore we can see the overall reaction equation is:

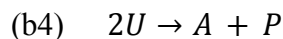


## The Oregonator

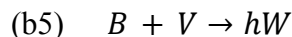
When attempting to model this reaction, the simplest model would be the Oregonator developed by Field and Noyes when they reduced their first proposed FKN mechanism to five coupled elementary stoichiometries (Field et al). The five equations are as follows, where  $A = BrO_3^-$ ,  $B = \text{malonic acid}$ ,  $P = HBrO$ ,  $U = HBrO_2$ ,  $V = Mn^{+3}$ , and  $W = Br^-$  (Steinbock et al). It must be noted that this model is intended to be used with the *cerium* ion catalyst, and the discrepancies between the experiment and the model will show in Section 6.3.







$$k_4 = (2 \cdot 10^3 \text{ mol}^{-1} \text{ dm}^3 \text{ s}^{-1})$$



$$k_5 = (0.3 \text{ mol}^{-1} \text{ dm}^3 \text{ s}^{-1})$$

The stoichiometric factor  $h$  is a crucial bifurcation parameter of the BZ reaction system (Steinbock et al). Its value, generally between 0.5 and 2, is determined through complex interactions between organic acid oxidations that result in higher  $[Br^-]$  (Steinbock et al). Each reaction is coupled with its corresponding rate constant derived at a temperature of 25 degrees celsius (Steinbock et al), with adjustments for the acidity of the solution. Based on these reaction mechanisms, the rate laws describing the concentrations of the intermediate species  $U$ ,  $V$ , and  $W$  can be derived. The concentrations of  $A$  and  $B$  are assumed to be constant due to both being present in high concentrations initially, replaced by  $a$  and  $b$  respectively, and  $P$  is irrelevant as an inert product.

$$(c1) \quad \frac{d[U]}{dt} = k_1 a[W] - k_2 [U][W] + k_3 a[U] - 2k_4 [U]^2$$

$$(c2) \quad \frac{d[V]}{dt} = 2k_3 a[U] - k_5 b[V]$$

$$(c3) \quad \frac{d[W]}{dt} = -k_1 a[W] - k_2 [U][W] + hk_5 b[V]$$

An attempt was made to solve these differential equations by hand, utilizing the integrated rate law and various approximations, including the standard state and pre-equilibrium approximations, though unfortunately none yielded supportive results. However, utilizing an ordinary differential equation solver, in this case Polymath Educational (Cutlip et al), a model could be constructed graphing the concentration of the Oregonator intermediates over time, which will be displayed in section 5.3.



# Method

The method of this experiment is split into two categories, one of preliminary preparations done during the process of diluting and creating the standard solutions used in each trial, and the procedure for the trials themselves. The trial procedure has been adapted from Shakhshiri's demonstration of the BZ reaction, which has been cross referenced with data from Jahnke and Winfree.

## Preliminary Preparations

1. A stock solution of  $KBrO_3$  and  $H_2SO_4$  was first prepared.  $180.0 \pm 0.5 \text{ cm}^3$  of  $H_2SO_4$  was diluted in  $1.820 \pm 0.005 \text{ dm}^3$  of deionised water, forming a concentration of  $1.62 \pm 0.01 \text{ mol dm}^{-3}$ .
2.  $19.95 \pm 0.01 \text{ g}$  of  $KBrO_3$  was then dissolved in the solution such that its concentration was  $0.0600 \pm 0.0002 \text{ mol dm}^{-3}$ . *Malonic acid* was not prepared in the large batch due to the concentration of *malonic acid* being varied across trials.

## Trial Procedure

1. Each trial was conducted at  $25.0 \pm 0.5$  degrees celsius, and  $50.0 \pm 0.5 \text{ cm}^3$  of the premade solution was poured into a  $150 \text{ cm}^3$  erlenmeyer flask.
2. The flask was set on a magnetic stirrer, with a speed such that a small vortex formed in the centre of the flask.
3. *Malonic acid* is then introduced to the solution, followed by  $0.13 \pm 0.1 \text{ g}$  of  $MnSO_4 \cdot H_2O$ , creating a  $[MnSO_4]$  of  $0.015 \pm 0.001$ .

4. Set up a video camera prior to each trial, such that at the beginning with the addition of  $MnSO_4 \cdot H_2O$ , subsequent oscillations are counted and measured following the initial red and clear periods of the solution. Each oscillation was counted at the first appearance of red following a clear solution, and each trial was recorded for approximately 13 oscillations before ending the footage and disposing of the solution.

Figure 3.0: Table of *malonic acid* masses with concentrations

Trial Number	Mass of $CH_2(COOH)_2$ ( $\pm 0.01$ g)	Initial Concentration ( $\pm 0.003$ mol dm <sup>-3</sup> )
1	0.31	0.060
2	0.42	0.081
3	0.52	0.100
4	0.62	0.119
5	0.73	0.140
6	0.83	0.160
7	0.94	0.181
8	1.04	0.200
9	1.14	0.219
10	1.25	0.240

## Results

Figure 4.0: Average of the initial 5 oscillations for concentrations 0.06 to 0.24  $\text{mol dm}^{-3}$

Concentration of $\text{CH}_2(\text{COOH})_2$ ( $\pm 0.004 \text{ mol dm}^{-3}$ )	Trial Set 1 ( $\pm 1 \text{ s}$ )	Trial Set 2 ( $\pm 1 \text{ s}$ )	Trial Set 3 ( $\pm 1 \text{ s}$ )
0.060	24	41	44
0.081	30	31	38
0.100	26	26	45
0.119	27	32	33
0.140	28	36	36
0.160	36	26	19
0.181	25	25	26
0.200	27	28	27
0.219	26	32	13
0.240	25	27	25

Figure 4.1: Average oscillations of all trial sets for concentrations 0.06 to 0.24  $\text{mol dm}^{-3}$

Concentration of $\text{CH}_2(\text{COOH})_2$ ( $\pm 0.004 \text{ mol dm}^{-3}$ )	Average Oscillation Time ( $\pm 1 \text{ s}$ )
0.060	36.4
0.081	33.3
0.100	32.4
0.119	30.7
0.140	33.4
0.160	27.1
0.181	25.3

0.200	27.5
0.219	23.5
0.240	25.9

## Sample Calculations

Sample calculation for the  $[CH_2(COOH)_2]$ .

$$[CH_2(COOH)_2] = \frac{0.31 \pm 0.01 \text{ g}}{(104.061 \pm 0.001 \text{ g mol}^{-1})(0.0500 \pm 0.0005 \text{ dm}^3)}$$

$$[CH_2(COOH)_2] = 0.060 \pm (0.060) \left( \frac{0.01}{0.31} + \frac{0.001}{104.061} + \frac{0.0005}{0.0500} \right) \text{ mol dm}^{-3}$$

$$[CH_2(COOH)_2] = 0.060 \pm 0.003 \text{ mol dm}^{-3}$$

Sample calculation for the dilution of concentrated  $H_2SO_4$ , subsequent addition of  $KBrO_3$ , and the initial  $[MnSO_4]$  of each trial.

$$[H_2SO_4] = \frac{(0.1800 \pm 0.0005 \text{ dm}^3)(18.00 \pm 0.01 \text{ mol dm}^{-3})}{2.000 \pm 0.005 \text{ dm}^3}$$

$$[H_2SO_4] = 1.62 \pm (1.62) \left( \frac{0.0005}{0.1800} + \frac{0.01}{18.00} + \frac{0.005}{2.000} \right) \text{ mol dm}^{-3}$$

$$[H_2SO_4] = 1.62 \pm 0.09 \text{ mol dm}^{-3}$$

$$[KBrO_3] = \frac{19.95 \pm 0.01 \text{ g}}{(166.189 \pm 0.001 \text{ g mol}^{-1})(2.000 \pm 0.005 \text{ dm}^3)}$$

$$[KBrO_3] = 0.06002 \pm (0.06002) \left( \frac{0.01}{19.95} + \frac{0.001}{166.189} + \frac{0.005}{2.000} \right) \text{ mol dm}^{-3}$$

$$[KBrO_3] = 0.0600 \pm 0.0002$$

$$[MnSO_4] = \frac{0.13 \pm 0.01 \text{ g}}{(169.009 \pm 0.001 \text{ g mol}^{-1})(0.0500 \pm 0.0005 \text{ dm}^3)}$$

$$[MnSO_4] = 0.015 \pm (0.015) \left( \frac{0.01}{0.13} + \frac{0.001}{169.009} + \frac{0.0005}{0.0500} \right) \text{ mol dm}^{-3}$$

$$[MnSO_4] = 0.015 \pm 0.001 \text{ mol dm}^{-3}$$

Sample calculation for the average oscillation time of the initial five oscillations of trial set 1 at

$0.060 \pm 0.004 \text{ mol dm}^{-3} [CH_2(COOH)_2]$ .

$$\overline{\text{initial 5 oscillations}} = \left( \frac{122 \pm 1 \text{ s}}{5} \right)$$

$$\overline{\text{initial 5 oscillations}} = 24.4 \pm (24.4) \left( \frac{1}{122} \right) \text{ s}$$

$$\overline{\text{initial 5 oscillations}} = 24.4 \pm 0.2 \text{ s}$$

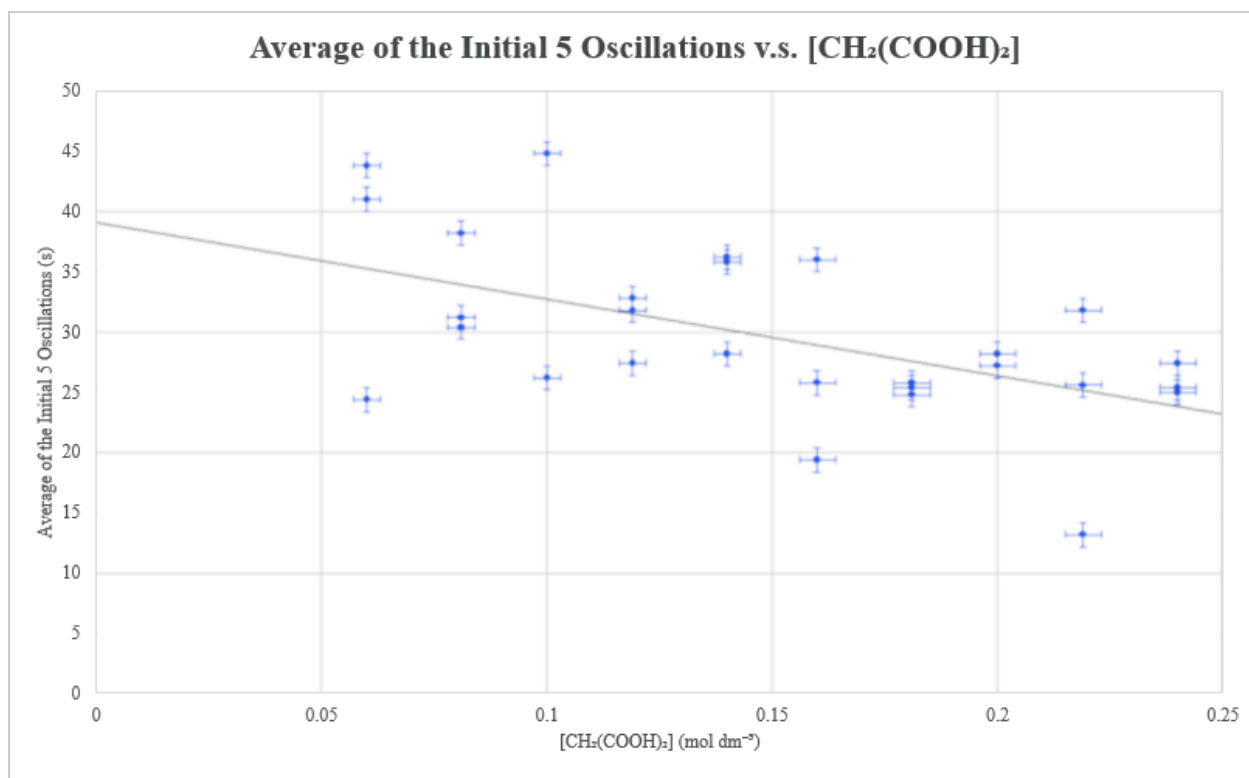
$$\overline{\text{initial 5 oscillations}} = 24 \pm 1 \text{ s}$$

# Analysis

Plotting figure 4.0 on a graph yields the following, with the linear trend line determined using linear regression. The number of averaged oscillations has been chosen as 5, due to oscillations remaining relatively stable within this time frame, allowing the assumption of a constant  $[BrO_3^-]$  and  $[CH_2(COOH)_2]$  when modeling.

Figure 5.0: Average of the initial 5 oscillations v.s. *malonic acid* concentration

Trend line:  $f(x) = \left(\frac{-127}{2}\right)x + 39.08$





## Pearson's Correlation Coefficient

Experimental results showed a decrease in the oscillation time, or an increase in reaction rate, as  $[CH_2(COOH)_2]$  increased. Utilizing Pearson's correlation coefficient, the statistical correlation of the results was analyzed. Substituting the data into the following equation, where  $r$  is the coefficient in question,  $x_i$  and  $y_i$  are individual data points indexed with  $i$ , and  $\bar{x}$  and  $\bar{y}$  are the averages, the coefficient was calculated using data from figure 4.0.

$$r = \frac{\sum_i^n (x_i - \bar{x})(y_i - \bar{y})}{\sqrt{\sum_i^n (x_i - \bar{x})^2} \sqrt{\sum_i^n (y_i - \bar{y})^2}}$$

$$r = -0.5414$$

The value of  $r$  is always between 1 and -1, and the closer to either of these values the stronger the respective positive or negative correlation. The value of  $r$  in this case signifies a moderate negative correlation. The significance of the data was calculated using Microsoft Excel, and the calculation returned 0.002022, showing that the probability of obtaining these results by chance is approximately 0.2%, allowing the null hypothesis to be rejected with a great amount of certainty. Conversely, an average between the trial sets can also be taken, with the resulting tables and charts shown in figure 4.1. The correlation coefficient in this case is -0.9049, which indicates an extremely strong correlation, with a statistical significance of 0.000317, or 0.03% certainty.

From equations (c1) through (c3), we observe that according to the elementary stoichiometries, the rate of change in  $[V]$  and  $[W]$  is dependent on the  $[CH_2(COOH)_2]$ . Therefore, while the data is not completely supportive of a negative relationship between  $[CH_2(COOH)_2]$

and the average of the initial 5 oscillations, it does agree with our initial hypothesis and background information. The data also demonstrates discrepancies between the error bars and the variation in average oscillation time will be expanded upon in section 6.1.

## Solution Acidity Adjustments

$[H^+]$  must be calculated to utilize the model, as some of the rate constants that describe the Orgeonator system are adjusted for the acidity of the reaction medium, as  $H^+$  is a participant in some parts of the mechanism. Due to  $H_2SO_4$  being a diprotic acid, it dissociates in two steps, and as  $HSO_4^-$  is a weak acid, one cannot treat  $H_2SO_4$  as releasing both protons or only one proton (Jahnke and Winfree). The  $[H^+]$  at 25°C can be calculated through the following equation, where  $(x + c)$  is the final  $[H^+]$ ,  $c$  is the initial  $[H_2SO_4]$ , and  $K$  is the equilibrium constant for the second dissociation step at 25°C, which has a value of  $10^{-1.92}$  (Jahnke and Winfree). While  $H^+$  actually exists in a dynamic equilibrium due to its participation in the BZ reaction, its fluctuation is not significant enough for this approximation of a constant  $[H^+]$  to be invalid.

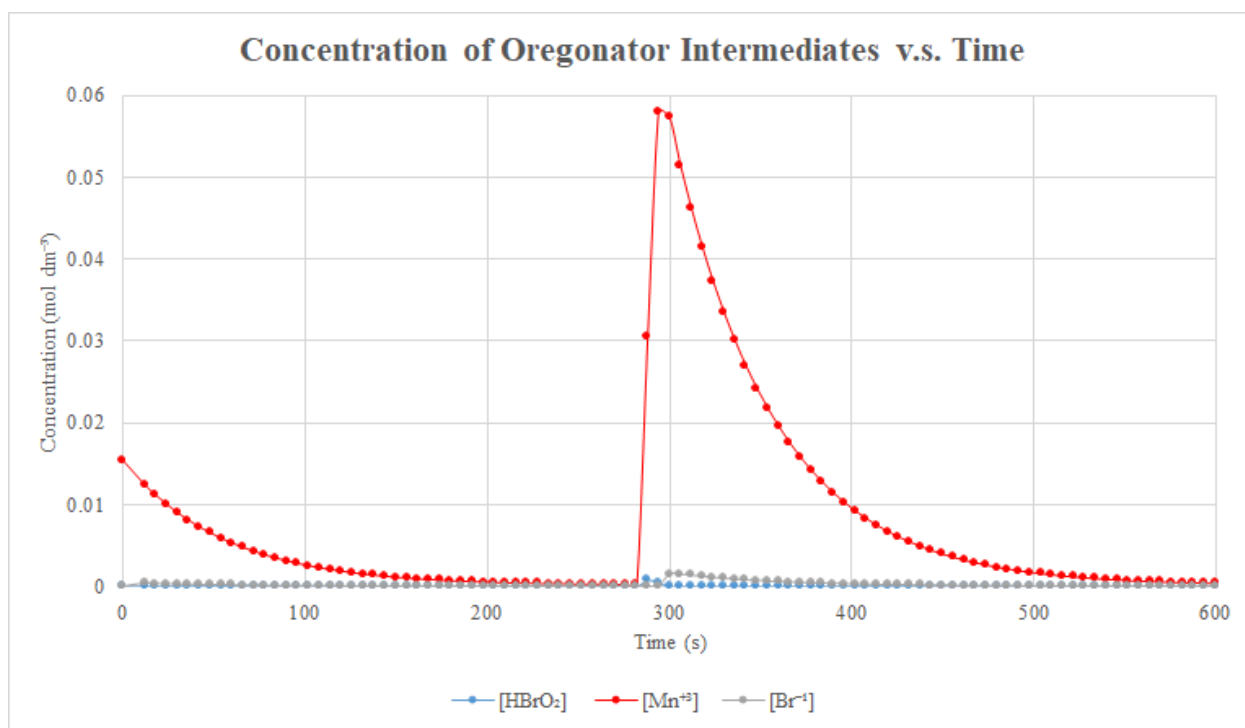
$$x = \frac{-(c + K) \pm \sqrt{(c + K)^2 + 4(K)(c)}}{2} + c$$

Replacing variables with known values of  $c$  and  $K$  yield  $[H^+]$  to be  $1.63 \pm 0.02 \text{ mol dm}^{-3}$ . This value is barely a significant departure from the concentration of  $H^+$  had the assumption been made that  $H_2SO_4$  is monoprotic, though this will improve the accuracy when modeling and considering the ramifications of the experimental data. While *malonic acid* is a weak acid and would partly dissociate to produce  $H^+$  as well, due to it being consumed by the BZ reaction, the equilibrium is in fact dynamic and cannot be accurately predicted.

## Oregonator Model Comparisons

Having solved for  $[H^+]$ , we can now model the reactions using an ordinary differential equation solver. Setting values of  $[CH_2(COOH)_2]$  to  $0.06 \text{ mol dm}^{-3}$  and initial  $[Mn^{+3}]$  to  $0.015 \text{ mol dm}^{-3}$ , we obtain the following graphs with the corresponding  $[Mn^{+3}]$  values for the concentration of Oregonator intermediates over a time interval of 10 minutes.

Figure 5.1: Concentration of oregonator intermediates over time,  $[CH_2(COOH)_2] = 0.06 \text{ mol dm}^{-3}$  (Cutlip et al)



Despite not reflecting experimental data, one may utilize this by comparing the oscillations between the  $[CH_2(COOH)_2]$  at  $0.06 \text{ mol dm}^{-3}$  and  $0.24 \text{ mol dm}^{-3}$ , and observe whether

the experimental relation holds true for the model, which is a negative relation between average oscillation time and  $[CH_2(COOH)_2]$ .

Figure 5.2: Concentration of oregonator intermediates over time,  $[CH_2(COOH)_2] = 0.24 \text{ mol dm}^{-3}$  (Cutlip et al)

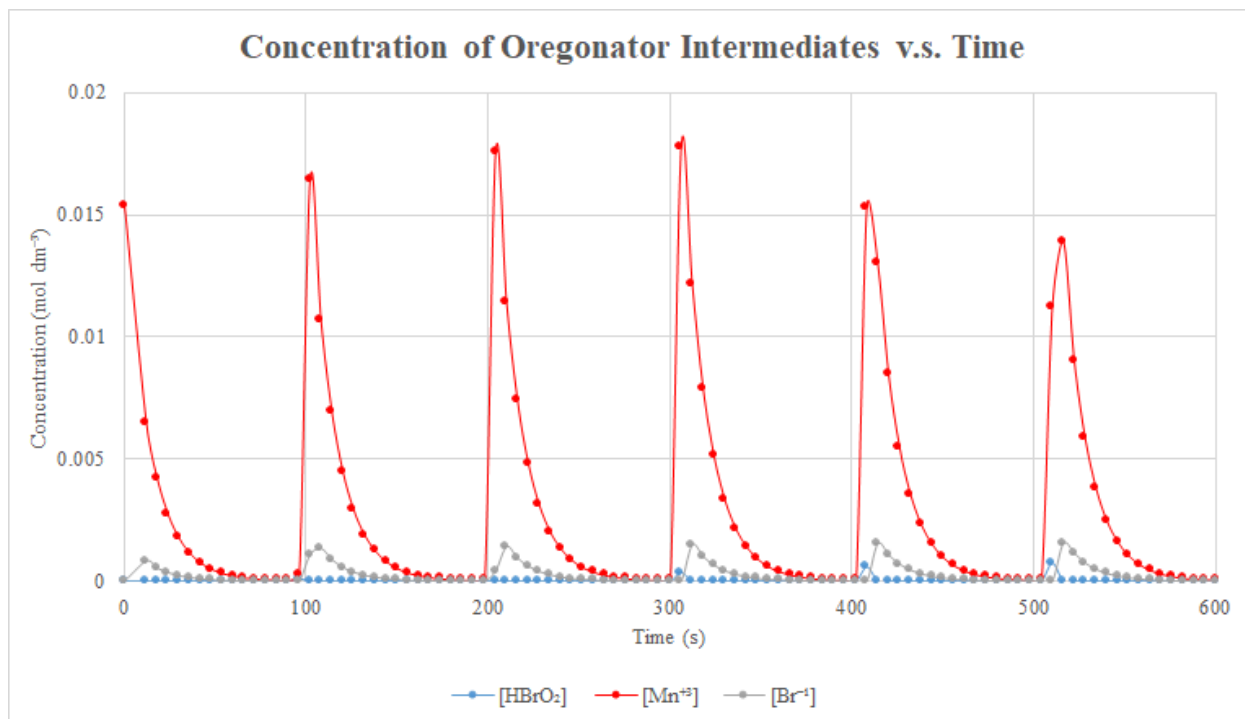


Figure 5.2 shows a clear increase in reaction rate, almost quintupling the rate of figure 5.1. However, the oscillation times displayed do not reflect experimental data, with dramatically slower modeled results. Experimental conditions such as temperature and pressure were kept the same as the source which reported  $k_1$  through  $k_5$  (Steinbock et al), thus it is not the conditions that cause this incongruence. One concludes this is likely due to limitations of the model, as the transition metal ion catalyst is anticipated as  $Ce^{+4}$  within the Oregonator, thus manganese may be likely to have different properties, being able to increase the reaction rate further than cerium.

Cerium forms a complex ion  $[Ce(H_2O)_9]^{+3}$  in its  $Ce^{+3}$  oxidation state, thereby denoting a coordination number of 9 (Winter). This is in contrast to  $Mn^{+2}$ , which forms  $[Mn(H_2O)_6]^{+2}$  with a coordination number of 6 (Clark). Therefore  $Ce^{+3}$  is a much larger molecule when aqueous, and the increased amount of water molecules in its vicinity could lead to increased repulsion from the other ions. This would cause  $BrO_3^-$  and  $HBrO_2$  to not react as readily with  $Ce^{+3}$ , reducing the likelihood of a collision with proper geometry. Körös discovered that BZ reactions behave as if there is a single rate-determining step, since it obeys the Arrhenius equation, yielding practically the same activation energy for all three catalysts (Bánsági et al), thus the only remaining contributor to a lower rate constant is the pre-exponential factor, which accounts for collisions between molecules and geometry.

Furthermore, aqueous  $Ce^{+4}$  is metastable in water, which may also affect its ability as a catalyst, thereby causing reaction rates to be much slower in general for cerium catalyzed systems (Mcgill). However,  $Ce^{+4}$  is also a strong oxidizing agent, which would seem to increase its tendency to react and oxidize *malonic acid* (Mcgill), though this may be insignificant in comparison to the relatively small ionic radius of  $Mn^{+3}$  and its higher reactivity as a result of that.

## Conclusions

This paper has demonstrated the relationship between the  $[CH_2(COOH)_2]$  and the average oscillation time of the manganese catalyzed BZ reaction. An increase in  $[CH_2(COOH)_2]$  corresponds to a decrease in average oscillation time, or an increase in reaction rate. Analysis was conducted through graphical techniques, where a linear trend line was fitted to a scatter plot of 30 data points, with moderate to strong negative correlation between the dependent and independent variables, supported by a model constructed of 5 coupled stoichiometries and an examination of the reaction mechanism. Furthermore, where discrepancies showed between the experiment and the model, an explanation based on complex ion interactions affecting rate and activity of the catalyst species due to molecular geometry differences was put forward.

## Error Analysis

As with all experiments, random error is present. In order to minimize its impact in future iterations, further repeat trials must be conducted to obtain larger sample sizes that can be averaged. In fact, a crucial error in not preparing the  $MnSO_4 \cdot H_2O$  in a large batch along with the  $BrO_3^-$  and sulfuric acid was made. The only reaction arising from the two reactants being in contact with each other would be the reduction of bromate, or process (a1) in section 3.1, which would not impede oscillations from developing. Preparation of reactants in large volumes would reduce random error due to less measurements and a significantly lower percentage error in concentration. However, large variations in the average oscillation time were observed, and this can only be due to a random error that has been unaccounted for so far. This may be due to the

fact that  $MnSO_4$  was added as a solid to the reaction solution, causing a delay as it had to dissolve first before participating in the reaction. This is not a systematic error, as it is too difficult to predict how it would affect the average oscillation when some  $MnSO_4$  is dissolved, and the rest eventually becomes aqueous as well. If the  $MnSO_4$  was introduced in aqueous form, with the obvious adjustments to solution volume and concentrations prior to the introduction of  $MnSO_4$ , this would have been mitigated.

The first instance of systematic error is within the method used in recording oscillation times. Instead of observing a change in color and simply counting and averaging, the reaction could have been run within a spectrophotometer, allowing for a direct observation of absorption of the solution over time, and since  $Mn^{+2}$  is coloured red, one could track its concentration by extension. This would allow for more precision and accuracy in observing oscillations, as one could simply record each individual oscillation by finding the difference in time between two peaks in absorption. This would also allow a direct comparison to the model, as the  $[Mn^{+2}]$  is inversely related to the  $[Mn^{+3}]$ .

There are disadvantages to using a spectrophotometer however. A cuvette of a  $1\text{ cm}^3$  capacity would be the reaction container, and due to the low volume of reactants one would expect the reactants to be depleted relatively quickly. Furthermore, separate solutions would have to be created for the  $Mn^{+2}$  ion and the rest of the reactants, since one could not mix the reactants together before transferring to a cuvette, as the oscillations would have already begun. Having separate solutions mixed together within a cuvette would significantly increase percentage error in volume measurements.

A second reduction in systematic error can be made, though unlikely due to the equipment necessary. A large issue with this experiment is the inability to maintain a constant concentration of *malonic acid*, causing a gradual decrease in reaction rate over time during experimental trials. This could be counteracted through the use of a continuous-flow stirred tank reactor, which could continuously inject reactants at a specified rate such that their concentration remains constant. This would bridge the gap between the model and the experiment, as it would render the assumption of the model true in the experimental case.



# Works Cited

- Bánsági Tamás, et al. "High-Frequency Oscillations in the Belousov-Zhabotinsky Reaction." *The Journal of Physical Chemistry A*, vol. 113, no. 19, 17 Mar. 2009, pp. 5644–5648., doi:10.1021/jp901318z.
- Britton, Melanie M. "Spatial Quantification of  $\text{Mn}^{2+}$  and  $\text{Mn}^{3+}$  Concentrations in the Mn-Catalyzed 1,4-Cyclohexanedione/Acid/Bromate Reaction Using Magnetic Resonance Imaging." *The Journal of Physical Chemistry A*, vol. 110, no. 8, 20 Jan. 2006, pp. 2579–2582., doi:10.1021/jp057201f.
- Clark, Jim. "Manganese." *Chemguide*, Apr. 2017, [www.chemguide.co.uk/inorganic/transition/manganese.html](http://www.chemguide.co.uk/inorganic/transition/manganese.html).
- Cutlip, Michael, et al. "Polymath-Software." *Polymath-Software*, [www.polymath-software.com/index.htm](http://www.polymath-software.com/index.htm).
- Epstein, Irving R., and John A. Pojman. *An Introduction to Nonlinear Chemical Dynamics: Oscillations, Waves, Patterns, and Chaos*. Oxford University Press, 1998.
- Field, Richard J., et al. "Oscillations in Chemical Systems. II. Thorough Analysis of Temporal Oscillation in the Bromate-Cerium-Malonic Acid System." *Journal of the American Chemical Society*, vol. 94, no. 25, 13 Dec. 1972, pp. 8649–8664., doi:10.1021/ja00780a001.
- Hill, Dan and Timothy Morgan. "Pattern Formation and Wave Propagation in the Belousov-Zhabotinskii Reaction." 2003.

Jahnke, Wolfgang, and Arthur T. Winfree. "Recipes for Belousov-Zhabotinsky Reagents."

*Journal of Chemical Education*, vol. 68, no. 4, 1991, pp. 320–324.,

doi:10.1021/ed068p320.

"Malonic Acid." *PubChem*, U.S. National Library of Medicine,

pubchem.ncbi.nlm.nih.gov/compound/Malonic-acid.

Mcgill, Ian. "Rare Earth Elements." *Ullmann's Encyclopedia of Industrial Chemistry*, 15 June

2000, doi:10.1002/14356007.a22\_607.

Shakhashiri, Bassam Z. *Chemical Demonstrations: A Handbook for Teachers of Chemistry*. Vol.

2, University of Wisconsin Press, 1985.

Steinbock, Oliver, et al. "Oxygen Inhibition of Oscillations in the Belousov–Zhabotinsky

Reaction." *The Journal of Physical Chemistry A*, vol. 104, no. 27, 25 Apr. 2000, pp.

6411–6415., doi:10.1021/jp000531.

Tyson, John J. *The Belousov-Zhabotinskii Reaction*. Springer-Verlag, 1976.

Winter, Mark. "Cerium: Reactions of Elements." *Cerium: Reactions of Elements*, The University

of Sheffield and WebElements, www.webelements.com/cerium/chemistry.html.

# Appendices

Figure 8.0: Table of modeled concentrations of Oregonator intermediates over time,

$[CH_2(COOH)_2] = 0.06 \text{ mol dm}^{-3}$  (Cutlip et al)

Time (s)	$[HBrO_2] \text{ (mol dm}^{-3} \cdot 10^{-7})$	$[Mn^{+3}] \text{ (mol dm}^{-3} \cdot 10^{-5})$	$[Br^{-I}] \text{ (mol dm}^{-3} \cdot 10^{-6})$
0	0	1538	0
12.001608	1.9714	1240.8	358.14
24.003947	1.9746	1001.4	288.96
36.008371	1.9785	808.49	233.04
48.011133	1.9835	653.07	187.99
60.010197	1.9896	527.89	151.71
72.004294	1.9973	427.07	122.48
84.018965	2.0068	345.71	98.89
96.006431	2.0188	280.31	79.93
108.01921	2.0337	227.52	64.62
120.00349	2.0523	185.1	52.32
132.03378	2.0757	150.81	42.36
144.0419	2.1051	123.26	34.36
156.05313	2.1422	101.09	27.91
168.08548	2.1893	83.241	22.71
180.09713	2.2493	68.934	18.53
192.00798	2.3254	57.552	15.18
204.06434	2.4251	48.341	12.45
216.07174	2.5553	41.05	10.26
228.08314	2.7289	35.303	8.4818
240.02405	2.9651	30.869	7.051
252.17269	3.3101	27.484	5.8584
264.24403	3.8567	25.148	4.854
276.09304	5.1563	23.981	3.8212
288.00036	8250.4	3043	0.4067
300.00038	1.9613	5730.3	1517.5
312.00033	1.9617	4618.8	1337.3

324.00056	1.9625	3723.1	1077.8
336.0007	1.9636	3001.5	868.64
348.00255	1.9649	2420	700.1
360.00106	1.9665	1951.6	564.35
372.00463	1.9685	1574	454.92
384.00295	1.9711	1270	366.79
396.00104	1.9742	1025	295.78
408.0086	1.9781	827.4	238.52
420.00835	1.9829	668.34	192.42
432.0045	1.9889	540.22	155.28
444.01489	1.9964	436.88	125.33
456.01507	2.0057	353.7	101.21
468.00009	2.0173	286.76	81.8
480.01405	2.0319	232.71	66.13
492.03359	2.0501	189.17	53.5
504.02792	2.0729	154.18	43.34
516.05824	2.1016	125.93	35.14
528.01458	2.1377	103.33	28.57
540.04427	2.1835	85.041	23.24
552.05095	2.2418	70.383	18.95
564.02361	2.3163	58.661	15.51
576.14385	2.4138	49.18	12.7
588.04291	2.539	41.775	10.48
600	2.7062	35.894	8.6672

Figure 8.0: Table of modeled concentrations of Oregonator intermediates over time,

$[CH_2(COOH)_2] = 0.24 \text{ mol dm}^{-3}$  (Cutlip et al)

Time (s)	$[HBrO_2] (\text{mol dm}^{-3} \cdot 10^{-7})$	$[Mn^{+3}] (\text{mol dm}^{-3} \cdot 10^{-5})$	$[Br^{-I}] (\text{mol dm}^{-3} \cdot 10^{-6})$
0	0	1538	0
12.00148	1.964	649.39	822.1
24.00301	1.972	274.91	347.5
36.01502	1.991	117.01	147

48.01908	2.036	50.57	62.65
60.03289	2.148	22.61	27.08
72.02715	2.44	10.97	12.11
84.06044	3.34	6.418	5.739
96.00256	1078	30.39	0.1246
108.0014	1.962	1067.6	1332.4
120.0001	1.966	451.23	571.4
132.0061	1.978	191.34	241.4
144.007	2.005	81.89	102.4
156.011	2.071	35.79	43.86
168.0244	2.238	16.43	19.16
180.039	2.692	8.463	8.752
192.0511	4.415	5.729	4.227
204.0003	1.969	1756	423.9
216.0012	1.963	741.3	938.9
228.0019	1.97	313.66	396.7
240.0066	1.987	133.4	167.9
252.0112	2.026	57.47	71.42
264.0147	2.123	25.52	30.79
276.0395	2.374	12.15	13.65
288.0705	3.115	6.828	6.402
300.0156	12.97	6.171	2.24
312.0005	1.961	1218.9	1475.9
324.0016	1.965	514.93	652.3
336.0039	1.975	218.24	275.6
348.0098	1.999	93.19	116.8
360.0124	2.057	40.55	49.91
372.0516	2.201	18.38	21.67
384.1065	2.59	9.226	9.787
396.0752	3.913	5.899	4.731
408.0011	6059	1530.3	1.113
420.0002	1.963	846.32	1070.3
432.0005	1.969	357.93	452.9
444	1.983	152.11	191.6

456.0164	2.018	65.29	81.36
468.0416	2.102	28.77	34.92
480.0793	2.319	13.48	15.37
492.0608	2.934	7.334	7.16
504.0553	6.428	5.724	3.278
516.0004	1.961	1391.7	1537.1
528.0002	1.964	587.8	744.7
540.0035	1.973	248.92	314.5
552.0103	1.994	106.11	133.2
564.0163	2.044	45.98	56.81
576.0599	2.17	20.65	24.57
588.1022	2.5	10.15	11.01
600	3.54	6.173	5.304